ACS OMEGA

http://pubs.acs.org/journal/acsodf

Article

Using Waste Tire-Derived Particles to Remove Benzene and *n*-Hexane by Dynamic and Static Adsorption

Tonghui Bao, Yuming Jing, Hongbo Wang, Rui Shan, and Ning Wang*

Cite This: *ACS Omega* 2023, 8, 4899−4905

Read Online

ACCESS | Metrics & More | Article Recommendations

ABSTRACT: Scrap tire rubber particles were used and evaluated to adsorb some gaseous volatile organic compounds (VOCs), such as benzene and *n*-hexane. The results present that the adsorption capacities were 0.18 and 0.072 mg/g for *n*-hexane and benzene, respectively, in the static adsorption mode; the effective adsorption may be attributed to the carbon black of the tire. The adsorption process is in accordance with the Freundlich isothermal model and Lagergren pseudo-first-order kinetic equation. Correspondingly, the adsorption process is multilayer adsorption analyzed by the intramolecular diffusion model. In the dynamic adsorption mode, the maximum adsorption efficiencies of *n*-hexane and benzene were 80.7 and 81%, respectively, at flow velocities of 0.1 L/min *n*-hexane and 0.2 L/min benzene.

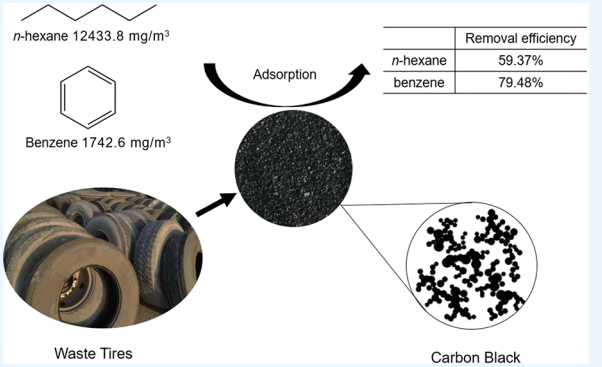

1. INTRODUCTION

The disposal and recycling of spent vehicle tires has become an issue due to the continuous development of the automobile industry and tension of landfilling space.[1] Waste tires are mainly composed of unbiodegradable rubber materials, occupying tremendous open land and breeding unpleasant mosquitoes and pathogens for a long time as well as easily causing fire if not being landfilled.[2] Rubber powder, refurbishments, recycled rubber, and pyrolysis are often used for tire disposal.[3−6] However, these methods either produce secondary pollution or fail to satisfy the treatment capacity. Previous studies have shown that waste tire particles could be used to adsorb environmental pollutants, including heavy-metal Cd^{2+} and Cu^{2+},[7,8] harmful organic matter,[9,10] arsenic in water environments,[11] oil spill,[12] and so on, which provides an alternative disposal option.

VOCs are important precursors of atmospheric ozone (O_3) and secondary organic aerosols, which cause atmospheric environmental problems such as haze and photochemical smog affecting human health[13] and becoming one of the key fields in environmental air research.[14−16] Adsorption,[17] chemical oxidation,[18] and biodegradation[19] are often used in practical treatment of VOCs. Among these methods, adsorption is considered to be a mature and effective one for VOC removal. The commonly used adsorbents are activated carbon, adsorption resin, modified starch adsorbents, modified cellulose adsorbents, and so on.[20−22] Unfortunately, they are too costly. Meanwhile, the rubber particles derived from waste tires have the advantages of low costs and stable physicochemical properties for adsorption.[23]

In this study, waste tire rubber particles were used as adsorbents for *n*-hexane and benzene, and the adsorption performance as gaseous VOC adsorbents was investigated by laboratory simulation of static adsorption, dynamic adsorption, adsorption kinetics, adsorption isotherm, and so on.

2. METHODOLOGY AND MATERIALS

2.1. Materials and Equipment. Two kinds of rubber particles are prepared. Type A is clean rubber particles with a small particle size and no impurities, and its particle density is measured to be 0.566 g/m^3. Type B has a larger particle size and some lint impurities, and its particle density is measured to be 0.473 g/m^3. In addition, sawdust with a particle size of 1−2 mm was prepared for the control experiment. Adsorbent materials are shown in Figure 1. Unfortunately, the IR spectra and XPS characterization were not satisfactory due to the mixed materials, large particle size, and presence of impurities.[24,25] VOCs are selected from benzene (Fuyu Fine Chemical Co., Ltd., Tianjin) and *n*-hexane (Comeo Reagent Co., Ltd., Tianjin), and the purity of benzene is of analytical purity, while the purity of *n*-hexane is of chromatographic purity.

Received: November 9, 2022
Accepted: January 19, 2023
Published: January 26, 2023

Figure 1. (a) Type A rubber particles. (b) Type B rubber particles. (c) Sawdust.

2.2. Static Adsorption. In the experiments, the flasks were full of hexane/benzene gas in certain concentrations and sealed with laboratory films (PM996, Parafilm M, Bemis Company, Inc., USA). Before each test, the VOC detector (MX6 composite gas detector, Industrial Scientific Corporation, USA) was calibrated and used to measure the background concentrations of the gas inside the conical flasks. A certain amount of rubber particles was quickly added and shaken for 10 min. At 10 min intervals, a total of 12 samples was gathered and measured. The process was triplicated for QA/QC.

2.3. Dynamic Adsorption. As shown in Figure 2, the experimental apparatus was assembled for the *n*-hexane/benzene adsorption experiment. The reaction column (PVC, h = 0.5 m, r = 25 mm) was washed with fresh air before each experiment to ensure a background VOC concentration of less than 5 ppm. During the experiments, air was pumped with an atmospheric sampler (QC-1S, Beijing Ke'an Labor Protective New Technology Company, Beijing) into the impinger containing liquid *n*-hexane/benzene to blow VOC vapors into the column. With a flow meter, the flow rate was controlled at 0.1 L/min for *n*-hexane and 0.02 L/min for benzene. A certain amount of rubber particles was placed into the column, and the outlet concentrations were continuously reported with the MX6 composite gas detector. The adsorption lasted for 40 min, and the data were derived and saved in a PC. The above steps were also triplicated.

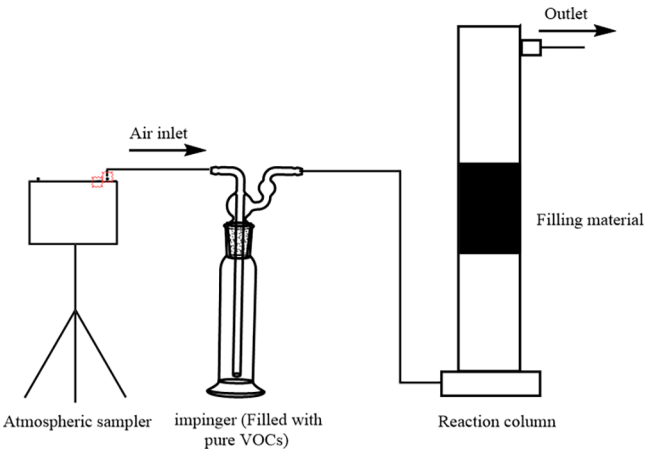

Figure 2. Schematic diagram of the dynamic test device connection.

Since the MX6 composite gas detector is designed to present values of isobutylene, they should be converted to the corresponding *n*-hexane/benzene as the following conversion relationship

$$C = \frac{M}{22.4} \times V \quad (1)$$

where the isobutylene unit of parts per million is turned into milligrams per cubic meter, C is the gas concentration (mg/m^3), M is the molecular weight of the measured gas (g/mol), and V is the measured volume concentration (ppm). Because the measured data is the isobutene concentration, M = 56.11 g/mol. According to the conversion relationship, the adsorption capacity of *n*-hexane is 4.06 times that of isobutene, and the adsorption amount of benzene is 0.55 times that of isobutene from which the adsorption capacity of *n*-hexane and benzene can be calculated.

3. RESULTS AND DISCUSSION

3.1. Static Adsorption. *3.1.1. Adsorption Ability of Different Rubber Particles.* Thirty grams of type A and type B rubber particles was tested to explore the adsorption capacity of *n*-hexane, and the results are shown in Figure 3.

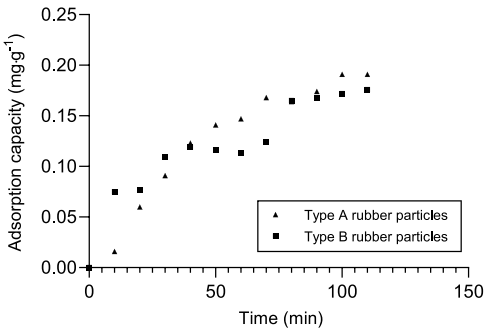

Figure 3. Static adsorption capacity of *n*-hexane by 30 g of two types of rubber particles.

During the first 30 min, type A rubber particles adsorbed less *n*-hexane than type B at the same mass, which is possibly due to the fact that the later rubber particles had a smaller density, allowing for a quicker contact between *n*-hexane gas and rubber particles at a short time. However, after 30 min, type A begins to adsorb more since the adsorption capacity of type B had been consumed. Eventually, the former rubber particles removed slightly more *n*-hexane at the end of the test (110 min). Due to the larger density, type A rubber particles possessed a smaller particle size and larger specific area for *n*-hexane gas in contact. Because the manufacture cost of type B

https://doi.org/10.1021/acsomega.2c07203
ACS Omega 2023, 8, 4899−4905

rubber particles was lower, they were used for the following experiments and called "rubber particles" only for writing convenience.

3.1.2. Adsorption of n-Hexane/Benzene on Rubber Particles. Thirty grams of type B rubber particles and sawdust were packed in the column for adsorption tests in the purpose of comparison. The adsorption capacities for *n*-hexane/benzene adsorption were monitored and calculated and are reported in Figure 4.

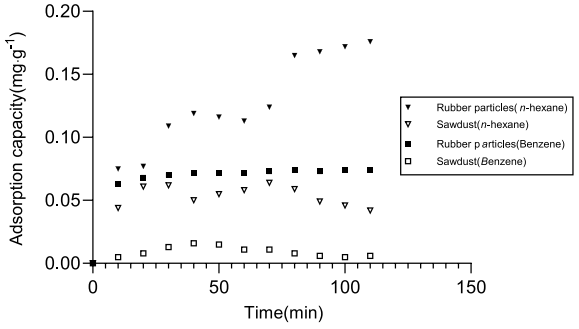

Figure 4. Static adsorption capacity of *n*-hexane and benzene by 30 g of rubber particles.

The rubber particles presented significant absorption of benzene and *n*-hexane compared to sawdust. However, it was noticed that the sawdust had a certain removal ability for *n*-hexane, which is possibly due to sawdust consisting of cellulose, hemicellulose, and lignin, which contain certain surface functional groups, for example, a hydroxyl group.[26]

At the end of the test, the adsorption quantity of rubber particles for *n*-hexane could reach 0.18 mg/g, while the value was approximately 0.05 mg/g for sawdust. The specific adsorption of benzene was approximately 72 mg/(g rubber particles) and only 0.008 mg/(g sawdust). The sawdust adsorbed less amounts of benzene than *n*-hexane, which is possibly due to the major components, namely, lignin and cellulose, which are polar molecules, repelling the nonpolar benzene.[27,28] In addition, a higher initial concentration of *n*-hexane could also lead to this phenomenon.

Regardless of whether by rubber particles or sawdust, more *n*-hexane was intercepted than benzene. The reason could be also attributed to different initial concentrations (*n*-hexane of 12,433.8 mg/m^3, while benzene of 1742.6 mg/m^3) and the molecular polarity. The adsorption rate presented a similar pattern for both gaseous organics, that is, fast at the beginning and then slowing down as the test proceeds. This is possibly due to the fact that the adsorption mostly occurred on the surface of rubber particles, and the active sites were quickly occupied, and the concentration of organic gas decreased as the process proceeded.[29,30]

As shown in Figure 5, the adsorption efficiencies of benzene were larger than *n*-hexane at different masses of rubber particles, and the adsorption efficiencies of both *n*-hexane and benzene increased with the increasing mass of rubber particles. When adding rubber particles of 50 g, the adsorption efficiency is as high as 79.48% of benzene with the *n*-hexane adsorption efficiency at 59.37%.

The Langmuir adsorption isotherm model is based on the formation of a monolayer adsorption on the surface of the adsorbent by a combination of adsorbates and limited sites. The Freundlich isotherm model is mainly applied to the adsorption process on inhomogeneous solid surfaces.

$$\frac{C_e}{q_e} = \frac{1}{K_L} + \frac{C_e}{q_{max}} \quad (2)$$

$$q_e = K_F C_e^{1/n} \quad (3)$$

where q_{max} is the maximum monolayer adsorption capacity (mg/g) and K_F and K_L are the adsorption constants for the two models, respectively. $1/n$ reflects the energy related to the adsorption process and the heterogeneity of the adsorbent; when $0.1 < 1/n < 1$, it means that the adsorption proceeds easily.[31]

Langmuir and Freundlich models were used to fit the adsorption isotherms of *n*-hexane and benzene. The adsorbed correlation coefficients (R^2) of the Langmuir isotherm model were 0.333 and 0.0164 for *n*-hexane and benzene on rubber particles, respectively. The adsorption process of rubber particles fits the Freundlich model well (Figure 6); parameters are shown in Table 1. It is shown that the adsorption process is multilayer adsorption, according to the Freundlich constant K_F; rubber particles have a satisfactory adsorption effect on the two gases, and *n*-hexane is better than benzene.[32,33]

3.2. Dynamic Adsorption. *3.2.1. n-Hexane.* During a continuous adsorption of *n*-hexane, 10, 20, and 30 g of rubber particles were packed and tested, and the results are presented in Figure 7. The adsorption of *n*-hexane reached a maximum in the range of 30−40 min; the peak adsorption capacities were 2991 mg/m^3 for 10 g of rubber particles, 7526 mg/m^3 for 20 g, and 9240.41 mg/m^3 for 30 g when the corresponding *n*-hexane removal efficiencies were 26.1, 65.7, and 80.7%, respectively.

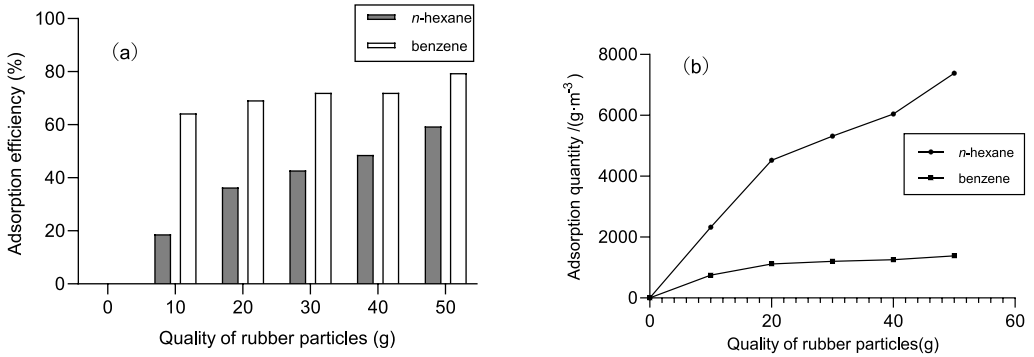

Figure 5. Adsorption (a) efficiency and (b) quantity of *n*-hexane and benzene by rubber particles with different masses under static adsorption equilibrium.

https://doi.org/10.1021/acsomega.2c07203
ACS Omega 2023, 8, 4899−4905

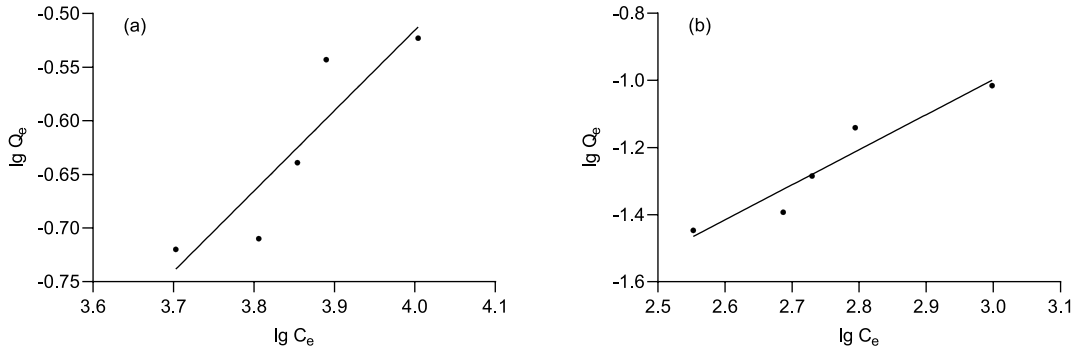

Figure 6. Freundlich adsorption isotherms of (a) *n*-hexane and (b) benzene at equilibrium in static adsorption.

Table 1. Fitting Results of Freundlich Adsorption Isotherm Related Parameters

	adsorption isotherm model		
category	K_F	$1/n$	R^2
rubber particles adsorbed *n*-hexane	0.2820	0.7503	0.8197
rubber particles adsorbed benzene	0.0161	1.0446	0.9182

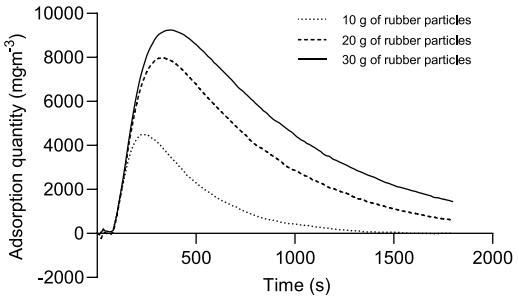

Figure 7. Dynamic testing of adsorbed *n*-hexane using 10, 20, and 30 g of rubber particles (mg/m^3).

The maximum specific dynamic adsorption was 0.591 mg/g for *n*-hexane on the same 30 g of rubber particles, which is larger than the value of static adsorption (0.18 mg/g). This may be due to the increased mass transfer in the dynamic adsorption process[34] and the fact that *n*-hexane had better contact with the rubber particles in dynamic adsorption.

3.2.2. Benzene. A similar continuous adsorption experiment was also conducted with benzene, and the maximum adsorption capacities were 292.07, 408.76, and 509.06 mg/m^3 on 10, 20, and 30 g of rubber particles, respectively (calculated based on Figure 8). The peak adsorption appeared at approximately 20 min.

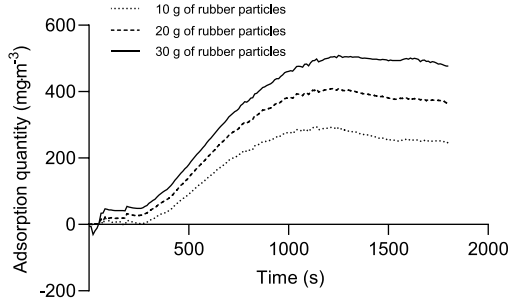

Figure 8. Dynamic testing of adsorbed benzene using 10, 20, and 30 g of rubber particles (mg/m^3).

Unlike *n*-hexane, the dynamic adsorption of benzene was slightly lower than the static adsorption on the same mass of rubber particles (0.059 vs 0.068 mg/g). This may be due to the fact that dynamic adsorption generates more heat of adsorption, which is not conducive to adsorption efficiency[35] and a lower liquefaction of benzene in the dynamic adsorption process.

Compared with the effect of dynamic adsorption of *n*-hexane by rubber particles, the effect of adsorption of benzene by rubber particles is close to that of *n*-hexane, which may be due to benzene and *n*-hexane being aromatic hydrocarbons, that is, straight chains with the same number of carbons and similar molecular weights.

3.3. Adsorption Kinetics. The adsorption kinetic model was used to determine the control mechanism of adsorption and to remove pollutants.[36] The results of the adsorption kinetics experiment for *n*-hexane on rubber particles are shown in Figure 9. The adsorption capacity of *n*-hexane increases with

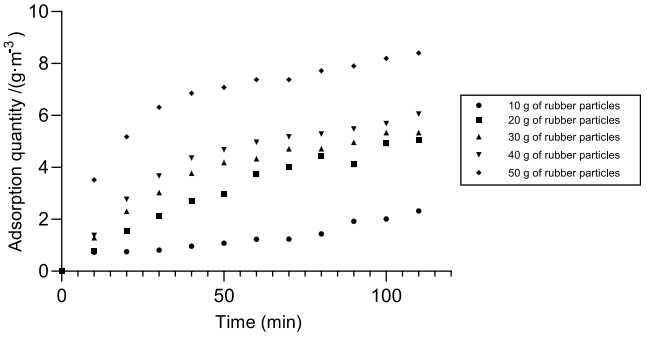

Figure 9. Static adsorption capacity of *n*-hexane with different-quality rubber particles (g/m^3).

time for various masses of rubber particles. Adsorption dynamic models were linearly fitted for the experimental data in Figure 10 with first-order and second-order kinetic equations.[37,38]

$$\ln(Q_e - Q_t) = \ln Q_e - k_1 t \quad (4)$$

$$\frac{t}{Q_e} = \frac{1}{k_2 Q_e^2} + \frac{t}{Q_e} \quad (5)$$

where Q_e (mg/g) is the adsorbed quantity of *n*-hexane at equilibrium, Q_t (mg/g) is the adsorbed quantity of *n*-hexane at time *t*, and k_1 and k_2 are the adsorption rate constants for the two models, respectively.

https://doi.org/10.1021/acsomega.2c07203
ACS Omega 2023, 8, 4899−4905

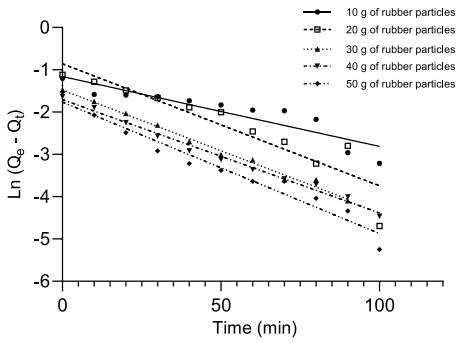

Figure 10. Calculation of the pseudo-first-order kinetic model for *n*-hexane static adsorption on rubber particles of differential quality.

As shown in Table 2, the adsorption of *n*-hexane by rubber particles conforms to the first-order kinetic model, and the R^2 values were relatively lower for 10 and 20 g, which is probably due to the low particle mass causing a significant wall interference. The model indicates that the adsorption of VOCs by rubber particles is controlled by diffusion and only one type of adsorption site on the surface of rubber granules.[39,40]

The intra-particle diffusion model shows that a linear line through the starting point of the drawing is provided, which indicates that the model discussed is the only speed-limiting step. As shown in Table 3, Q_t and $t_{1/2}$ have a good linear relationship but do not pass through the origin, implying that the adsorption process is affected by other speed-limiting steps except for the diffusion resistance in the particles.[41,42] The maximum internal diffusion rate constant is achieved at 20 g due to the more adequate contact with the adsorbed gas.

$$Q_t = K_p t^{1/2} + C \quad (6)$$

where Q_t (mg/g) is the adsorbed quantity of *n*-hexane at time *t*, K_p is the model rate constant, and *C* is the constant involving the boundary and thickness layers.

4. CONCLUSIONS

In this paper, the adsorption effects of waste rubber particles on two kinds of VOCs were analyzed by static adsorption and dynamic adsorption experiments. Static adsorption experiments show that the saturated adsorption capacities of *n*-hexane and benzene per unit mass of rubber particles are 0.18 and 0.072 mg/g, respectively, and the effect is much better than that of sawdust. Meanwhile, the similar adsorption capacity of the type A and type B rubber particles was verified by the comparative experiments. The adsorption process is in accordance with the Freundlich isothermal adsorption model and Lagergren pseudo-first-order kinetic equation. At the same time, the adsorption process does not conform to the intra-particle diffusion model, and the adsorption process is also affected by other factors. In the dynamic adsorption, the concentration of *n*-hexane in the reaction column is 2507.01 mg/m^3, the adsorption capacity of rubber particles to *n*-hexane is 0.591 mg/g, the concentration of benzene in the reaction column is 105.61 mg/m^3, and the adsorption capacity of rubber particles to benzene is 0.059 mg/g. Tire rubber particles are mainly composed of polymer (about 60−65%), carbon black (about 25−35%), and other additives;[43] the adsorption of VOCs may be attributed to the carbon black due to physical adsorption.[44,45] However, due to the complex composition of tire particles, the adsorption mechanism still needs to be verified. As a result, the significant adsorption effect is revealed by the adsorption of two gases by rubber particles, while their low price and high stability make them a promising adsorbent for VOCs.

Table 3. Intra-particle Diffusion Model of Rubber Particles Adsorbing *n*-Hexane

	particle diffusion model				
rubber particles	10 g	20 g	30 g	40 g	50 g
R^2	0.3034	0.9608	0.9489	0.8945	0.8707
intercept	−0.0054	−0.0013	−0.0003	−0.0005	0.0007
K_p	0.0012	0.0015	0.0006	0.0004	0.0004

AUTHOR INFORMATION

Corresponding Author

Ning Wang − *School of Municipal and Environmental Engineering and Resources and Environment Innovation Institute, Shandong Jianzhu University, Jinan 250101, P.R. China;* orcid.org/0000-0003-1738-9924; Email: wangning@sdjzu.edu.cn

Authors

Tonghui Bao − *School of Municipal and Environmental Engineering, Shandong Jianzhu University, Jinan 250101, P.R. China*

Yuming Jing − *School of Environment Science and Engineering, Shandong University, Qingdao 266237, P.R. China; Shandong Huankeyuan Environmental Engineering Co., Ltd, Jinan 250013, P.R. China*

Hongbo Wang − *School of Municipal and Environmental Engineering and Resources and Environment Innovation Institute, Shandong Jianzhu University, Jinan 250101, P.R. China*

Table 2. First-Order Kinetic and Second-Order Kinetic Simulations of *n*-Hexane Removal from Rubber Particles

	rubber particle quality	fitting equation	*K*	Q_e(mg/g)	R^2
first-order kinetics model	10 g	$Y = -0.01651X - 1.160$	0.01651	0.313	0.8277
	20 g	$Y = -0.02885X - 0.8584$	0.02885	0.424	0.8527
	30 g	$Y = -0.02866X - 1.480$	0.02866	0.228	0.9906
	40 g	$Y = -0.02678X - 1.706$	0.02678	0.182	0.9901
	50 g	$Y = -0.03106X - 1.764$	0.03106	0.171	0.9554
second-order kinetics model	10 g				0.0289
	20 g				0.0673
	30 g				<0
	40 g				0.0787
	50 g				0.0989

https://doi.org/10.1021/acsomega.2c07203
ACS Omega 2023, 8, 4899−4905

Rui Shan − *Guangzhou Institute of Energy Conversion, Chinese Academy of Sciences, Guangzhou 510640, P.R. China;* orcid.org/0000-0002-6181-0061

Complete contact information is available at: https://pubs.acs.org/10.1021/acsomega.2c07203

Funding

Natural Science Foundation of Shandong Province (grant no. ZR2020ME228); Key Technology Research and Development Program of Shandong (grant no. 2022CXGC021001); Introduction and Cultivation Plan for Young Innovative Talents of Colleges and Universities.

Notes

The authors declare no competing financial interest.

■ ACKNOWLEDGMENTS

We are grateful for the financial support provided by the Natural Science Foundation of Shandong Province (grant no. ZR2020ME228), Key Technology Research and Development Program of Shandong (grant no. 2022CXGC021001), and Introduction and Cultivation Plan for Young Innovative Talents of Colleges and Universities for this manuscript.

■ REFERENCES

(1) Ramarad, S.; Khalid, M.; Ratnam, C. T.; Chuah, A. L.; Rashmi, W. Waste tire rubber in polymer blends: A review on the evolution, properties and future. *Prog. Mater. Sci.* **2015**, *72*, 100.

(2) Alsaleh, A.; Sattler, M. L. Waste Tire Pyrolysis: Influential Parameters and Product Properties. *Curr. Sustainable/Renewable Energy Rep.* **2014**, *1*, 129−135.

(3) Cao, X.-W.; Luo, J.; Cao, Y.; Yin, X.-C.; He, G.-J.; Peng, X.-F.; Xu, B.-P. Structure and properties of deeply oxidized waster rubber crumb through long time ozonization. *Polym. Degrad. Stab.* **2014**, *109*, 1.

(4) Cataldo, F.; Ursini, O.; Angelini, G. Surface oxidation of rubber crumb with ozone. *Polym. Degrad. Stab.* **2010**, *95*, 803.

(5) Rijo, B.; Dias, A. P. S.; Wojnicki, Ł. Catalyzed pyrolysis of scrap tires rubber. *J. Environ. Chem. Eng.* **2022**, *10*, No. 107037.

(6) Yuhan, P.; Pingan, H.; Zhiliang, X.; Xinwen, W.; Yonggang, Z.; Qunxing, H. The effect of secondary reaction on volatiles composition during pyrolysis treatment of scrap tires. *Environ. Technol.* **2022**, 4054.

(7) Entezari, M. H.; Ghows, N.; Chamsaz, M. Ultrasound facilitates and improves removal of Cd(II) from aqueous solution by the discarded tire rubber. *J. Hazard. Mater.* **2006**, *131*, 84.

(8) Boongoi, P.; Opaprakasit, M.; Boondamnoen, O. Waste tire rubber as heavy metal ion adsorbent. *J. Phys.: Conf. Ser.* **2022**, *2175*, No. 012030.

(9) Lisi, R. D.; Park, J. K.; Stier, J. C. Mitigating nutrient leaching with a sub-surface drainage layer of granulated tires. *Waste Manage.* **2004**, *24*, 831.

(10) Islam, M. T.; Saenz-Arana, R.; Hernandez, C.; Guinto, T.; Ahsan, M. A.; Bragg, D. T.; Wang, H.; Alvarado-Tenorio, B.; Noveron, J. C. Conversion of waste tire rubber into a high-capacity adsorbent for the removal of methylene blue, methyl orange, and tetracycline from water. *J. Environ. Chem. Eng.* **2018**, *6*, 3070.

(11) Purakayastha, P. D.; Pal, A.; Bandyopadhyay, M. Sorption kinetics of anionic surfactant on to waste tire rubber granules. *Sep. Purif. Technol.* **2005**, *46*, 129.

(12) Lin, C.; Huang, C.-L.; Shern, C.-C. Recycling waste tire powder for the recovery of oil spills. *Resour., Conserv. Recycl.* **2008**, *52*, 1162.

(13) Mudliar, S.; Giri, B.; Padoley, K.; Satpute, D.; Dixit, R.; Bhatt, P.; Pandey, R.; Juwarkar, A.; Vaidya, A. Bioreactors for treatment of VOCs and odours − A review. *J. Environ. Manage.* **2010**, *91*, 1039.

(14) Zhang, Z.; Jiang, Z.; Shangguan, W. Low-temperature catalysis for VOCs removal in technology and application: A state-of-the-art review. *Catal. Today* **2016**, *264*, 270.

(15) Moufawad, T.; Gomes, M. C.; Fourmentin, S. Deep eutectic solvents as absorbents for VOC and VOC mixtures in static and dynamic processes. *Chem. Eng. J.* **2022**, *448*, No. 137619.

(16) Harrison, R. M.; Allan, J.; Carruthers, D.; Heal, M. R.; Lewis, A. C.; Marner, B.; Murrells, T.; Williams, A. Non-exhaust vehicle emissions of particulate matter and VOC from road traffic: A review. *Atmos. Environ.* **2021**, *262*, No. 118592.

(17) Wei, Q.; Yang, J.; Tian, C.; Zhang, Z.; Zhang, X.; Zhang, Z.; Li, D. Research on the Progress of VOCs Adsorption by Biomass Nanocomposites. *J. Phys.: Conf. Ser.* **2022**, *2194*, No. 012023.

(18) Attia, M. F.; Swasy, M. I.; Ateia, M.; Alexis, F.; Whitehead, D. C. Periodic mesoporous organosilica nanomaterials for rapid capture of VOCs. *Chem. Commun.* **2020**, *56*, 607.

(19) Roman, P.; Bijmans, M. F.; Janssen, A. J. Influence of methanethiol on biological sulphide oxidation in gas treatment system. *Environ. Technol.* **2016**, *37*, 1693.

(20) Su, C.; Guo, Y.; Chen, H.; Zou, J.; Zeng, Z.; Li, L. VOCs adsorption of resin-based activated carbon and bamboo char: Porous characterization and nitrogen-doped effect. *Colloids Surf., A* **2020**, *601*, No. 124983.

(21) Liu, H.; Xu, B.; Wei, K.; Yu, Y.; Long, C. Adsorption of low-concentration VOCs on various adsorbents: Correlating partition coefficient with surface energy of adsorbent. *Sci. Total Environ.* **2020**, *733*, No. 139376.

(22) Santos-Clotas, E.; Cabrera-Codony, A.; Ruiz, B.; Fuente, E.; Martín, M. J. Sewage biogas efficient purification by means of lignocellulosic waste-based activated carbons. *Bioresour. Technol.* **2019**, *275*, 207.

(23) Mora, P.; Alarcón, A.; Sánchez-Martín, L.; Llamas, B. Biomass Content in Scrap Tires and Its Use as Sustainable Energy Resource: A CO2 Mitigation Assessment. *Sustainability* **2021**, *13*, 3500.

(24) Wang, N.; Park, J.; Evans, E. A.; Ellis, T. G. Characterization of recycled rubber media for hydrogen sulphide (H2S) control. *Environ. Technol.* **2014**, *35*, 17−2505.

(25) Wang, N.; Park, J.; Ellis, T. G. The mechanism of hydrogen sulfide adsorption on fine rubber particle media (FRPM). *J. Hazard. Mater.* **2013**, *260*, 921.

(26) Mallakpour, S.; Sirous, F.; Hussain, C. M. Sawdust, a versatile, inexpensive, readily available bio-waste: From mother earth to valuable materials for sustainable remediation technologies. *Adv. Colloid Interface Sci.* **2021**, *295*, No. 102492.

(27) Chio, C.; Sain, M.; Qin, W. Lignin utilization: A review of lignin depolymerization from various aspects. *Renewable Sustainable Energy Rev.* **2019**, *107*, 232.

(28) Grunin, Y. B.; Grunin, L. Y.; Masas, D. S.; Talantsev, V. I.; Sheveleva, N. N. Proton magnetic relaxation study of the thermodynamic characteristics of water adsorbed by cellulose fibers. *Russ. J. Phys. Chem. A* **2016**, *90*, 2249.

(29) Xu, R.-k.; Xiao, S.-c.; Yuan, J.-h.; Zhao, A.-z. Adsorption of methyl violet from aqueous solutions by the biochars derived from crop residues. *Bioresour. Technol.* **2011**, *102*, 10293.

(30) Kim, Y.; Bae, J.; Park, H.; Suh, J.-K.; You, Y.-W.; Choi, H. Adsorption dynamics of methyl violet onto granulated mesoporous carbon: Facile synthesis and adsorption kinetics. *Water Res.* **2016**, *101*, 187.

(31) Liu, R.; Zhang, B.; Mei, D.; Zhang, H.; Liu, J. Adsorption of methyl violet from aqueous solution by halloysite nanotubes. *Desalination* **2011**, *268*, 111.

(32) Jain, M.; Khan, S. A.; Sahoo, A.; Dubey, P.; Pant, K. K.; Ziora, Z. M.; Blaskovich, M. A. Statistical evaluation of cow-dung derived activated biochar for phenol adsorption: Adsorption isotherms, kinetics, and thermodynamic studies. *Bioresour. Technol.* **2022**, *352*, No. 127030.

(33) Zhang, X.; Shang, H.; Yang, J.; Li, L.; Li, J. Nitrogen rejection from low quality natural gas by pressure swing adsorption experiments and simulation using dynamic adsorption isotherms. *Chin. J. Chem. Eng.* **2022**, *42*, 120.

(34) Liu, F.; Sai, K. C. K. V.; Zhang, W. Conversion of Spiky Sweetgum tree (Liquidambar styraciflua) Seeds as into Bio-adsorbent:

Static and Dynamic Adsorption Assessment. *J. Hazard. Mater. Adv.* **2021**, *1*, No. 100001.
(35) McDonough, J. R.; Law, R.; Reay, D. A.; Zivkovic, V. Intensified carbon capture using adsorption: Heat transfer challenges and potential solutions. *Therm. Sci. Eng. Prog.* **2018**, *8*, 17.
(36) Nourmoradi, H.; Nikaeen, M.; Khiadani, M. Removal of benzene, toluene, ethylbenzene and xylene (BTEX) from aqueous solutions by montmorillonite modified with nonionic surfactant: Equilibrium, kinetic and thermodynamic study. *Chem. Eng. J.* **2012**, *191*, 341.
(37) Hameed, B. H.; Daud, F. B. M. Adsorption studies of basic dye on activated carbon derived from agricultural waste: Hevea brasiliensis seed coat. *Chem. Eng. J.* **2008**, *139*, 48.
(38) Zhang, Z.; O'Hara, I. M.; Kent, G. A.; Doherty, W. O. S. Comparative study on adsorption of two cationic dyes by milled sugarcane bagasse. *Ind. Crops Prod.* **2013**, *42*, 41.
(39) Wang, Y.; Memon, M. Z.; Xie, Q.; Gao, Y.; Li, A.; Fu, W.; Wu, Z.; Dong, Y.; Ji, G. Study on CO2 sorption performance and sorption kinetics of Ce- and Zr-doped CaO-based sorbents. *Carbon Capture Sci. Technol.* **2022**, *2*, No. 100033.
(40) Amin, M. M.; Bina, B.; Rahimi, A.; Heidari, M. Adsorption of gas-phase n-hexane and benzene, toluene, ethyl benzene, and xylene onto compost; kinetics and isothermal studies. *Int. J. Environ. Health Eng.* **2015**, *4*, 27.
(41) Álvarez-Gutiérrez, N.; Gil, M. V.; Rubiera, F.; Pevida, C. Kinetics of CO2 adsorption on cherry stone-based carbons in CO2/CH4 separations. *Chem. Eng. J.* **2017**, *307*, 249.
(42) Rashidi, N. A.; Yusup, S.; Borhan, A.; Loong, L. H. Experimental and modelling studies of carbon dioxide adsorption by porous biomass derived activated carbon. *Clean Technol. Environ. Policy* **2014**, *16*, 1353.
(43) Leung, D. Y. C.; Wang, C. L. Kinetic study of scrap tyre pyrolysis and combustion. *J. Anal. Appl. Pyrolysis* **1998**, *45*, 153.
(44) Han, H.; Lee, J.; Park, D. W.; Shim, S. E. Surface Modification of Carbon Black by Oleic Acid for Miniemulsion Polymerization of Styrene. *Macromol. Res.* **2010**, *18*, 435.
(45) Douillard, J. M.; Pougnet, S.; Faucompre, B.; Partyka, S. The adsorption of polyoxyethylenated octyl and nonylphenol surfactants on carbon black and sulfur from aqueous solutions. *J. Colloid Interface Sci.* **1992**, *154*, 113.

https://doi.org/10.1021/acsomega.2c07203
ACS Omega 2023, 8, 4899−4905